

Article

Energy Consumption Modeling for Heterogeneous Internet of Things Wireless Sensor Network Devices: Entire Modes and Operation Cycles Considerations

Canek Portillo ^{1,*}, Jorge Martinez-Bauset ², Vicent Pla ² and Vicente Casares-Giner ²¹ Facultad de Ingeniería, Universidad Autónoma de Sinaloa, Ciudad Universitaria s/n, Culiacán 80013, Mexico² Departament of Communications, Universitat Politècnica de València (Technical University of Valencia), Camí de Vera s/n, 46022 València, Spain; jmartinez@upv.es (J.M.-B.); vpla@upv.es (V.P.); vcasares@upv.es (V.C.-G.)

* Correspondence: canekportillo@uas.edu.mx

Abstract: Wireless sensor networks (WSNs) and sensing devices are considered to be core components of the Internet of Things (IoT). The performance modeling of IoT-WSN is of key importance to better understand, deploy, and manage this technology. As sensor nodes are battery-constrained, a fundamental issue in WSN is energy consumption. Additional issues also arise in heterogeneous scenarios due to the coexistence of sensor nodes with different features. In these scenarios, the modeling process becomes more challenging as an efficient orchestration of the sensor nodes must be achieved to guarantee a successful operation in terms of medium access, synchronization, and energy conservation. We propose a novel methodology to determine the energy consumed by sensor nodes deploying a recently proposed synchronous duty-cycled MAC protocol named Priority Sink Access MAC (PSA-MAC). We model the operation of a WSN with two classes of sensor devices by a pair of two-dimensional Discrete-Time Markov Chains (2D-DTMC), determine their stationary probability distribution, and propose new expressions to compute the energy consumption based solely on the obtained stationary probability distribution. This new approach is more systematic and accurate than previously proposed ones. The new methodology to determine energy consumption takes into account different specific features of the PSA-MAC protocol as: (i) the synchronization among sensor nodes; (ii) the *normal* and *awake* operation cycles to ensure synchronization among sensor nodes and energy conservation; (iii) the two periods that compose a full operation cycle: the *data* and *sleep* periods; (iv) two transmission schemes, SPT (single packet transmission) and APT (aggregated packet transmission) (v) the support of multiple sensor node classes; and (vi) the support of different priority assignments per class of sensor nodes. The accuracy of the proposed methodology has been validated by an independent discrete-event-based simulation model, showing that very precise results are obtained.

Keywords: internet of things; wireless sensor network; WSN MAC protocols; energy consumption modeling



Citation: Portillo, C.; Martinez-Bauset, J.; Pla, V.; Casares-Giner, V. Energy Consumption Modeling for Heterogeneous Internet of Things Wireless Sensor Network Devices: Entire Modes and Operation Cycles Considerations. *Telecom* **2024**, *5*, 723–746. <https://doi.org/10.3390/telecom5030036>

Academic Editor: Barbara M. Masini

Received: 23 May 2024

Revised: 24 June 2024

Accepted: 1 July 2024

Published: 2 August 2024



Copyright: © 2024 by the authors. Licensee MDPI, Basel, Switzerland. This article is an open access article distributed under the terms and conditions of the Creative Commons Attribution (CC BY) license (<https://creativecommons.org/licenses/by/4.0/>).

1. Introduction

The development of the Internet of Things (IoT) has been fueled by the growth of smart systems and WSN technologies. In fact, wireless sensor nodes (SNs) are considered to be core components of the IoT [1]. Several examples of WSN-based IoT applications could be described. In precision agriculture applications, SNs are spread over the field to sense the soil moisture, temperature, and humidity [2]. In IoT-based environmental applications, SNs continuously monitor the environment and send an alert signal if an emergency event is detected [3]. Also, in the Industrial Internet of Things (IIoT), the focus is on processes automation by proper data collection and communication among SNs, actuators, and processing units [4].

As SNs are energy-constrained devices, a substantial research effort has been devoted to finding solutions that contribute to the optimization of energy consumption. In [5], a software-based information-processing approach has been followed, while in [6], a combination of software and hardware-based approaches have been proposed to reduce energy consumption and meet certain maintenance requirements. To extend the WSN lifetime, energy conservation has also been studied from other perspectives as communication protocols, routing algorithms, Medium Access Control (MAC) schemes, and packet aggregation schemes [7–9].

Considering that energy conservation is a key factor, the modeling and analysis of energy consumption is of fundamental importance to better understand, manage, and design IoT WSNs. To this end, several models have been proposed to analyze energy consumption in WSN networks for IoT applications. For example, in [10], a very detailed deterministic model is developed, where a simple MAC is considered, focusing more on the consumption of the physical layer and considering three operating modes.

In [11], the authors present a stochastic model, where the energy consumption is modeled as a random variable with a given probability distribution, as well as maximum and minimum expected energy values. The model mainly takes into account physical layer issues, while a relatively simple MAC is used. Physical layer and routing issues are studied in [12]. A stochastic model is proposed to evaluate different topologies. Different random variables and their corresponding probability distributions are used to model communication hops between SNs, distances, and the number of SNs in the network. The analytical model is validated by simulation. However, the model uses a generic MAC protocol that is not even specified.

Different studies rely on Markov chains to model and analyze the energy consumption in WSNs [13] and to predict the energy consumed by SNs [14]. These models determine the energy consumed by an SN considering how a packet transmission evolves through different states. However, only very basic MAC features are incorporated into the models. In [15], the model of a WSN is presented, where SNs deploy a generic synchronous duty-cycle (SDC)-based MAC protocol. To determine the energy consumption, two principal operating periods for SNs are considered, the sleep as well as the other two additional intermediate periods. Their authors used a joint probability distribution to model the number of data packets and a multidimensional Markov process to model the SN phases. However, no specific MAC protocol or any synchronization scheme is incorporated into the model.

We claim that the MAC protocol is a fundamental part of a WSN and, therefore, it must be considered by any model aimed at evaluating its performance and energy consumption. Depending on traffic conditions and SN density, the nature of the contention to access a shared medium leads to conflicting events that can lead to packet collisions and have a great impact on the network performance, as well as on the energy consumed by SNs [16]. The studies mentioned above have in common that they only consider very basic MAC features, if any, and the impact of collisions was not considered. In addition, neither SN heterogeneity nor priority assignments were considered.

To determine energy consumption in the above models, different operational states of a SN were defined. However, the models consider that states of SNs in a WSN are independent of each other, i.e., the energy consumed by a sensor is not influenced by the states of the rest of the SNs of the WSN. In our opinion this simplifying assumption does not hold in real scenarios. Clearly, the access to a shared medium leads to a certain degree of dependency among the SN states, and consequently, it has an important impact on the energy consumed by SNs. Moreover, if we consider heterogeneous scenarios where multiple SN classes exist, possibly with different access priorities and different transmission schemes, such as SPT and APT, an accurate model to determine energy consumption should incorporate all these features, as they also have a great impact on network operation, performance, and energy consumption.

Other studies that focus on computing energy consumption in WSNs have deployed approaches similar to the ones proposed in our study. For example, in [17], a stochastic analysis of the energy consumption based on DTMCs is proposed. However, they consider neither heterogeneous scenarios nor an APT scheme.

In [18], an energy analysis of a WSN based on DTMCs is presented. It also considers an APT scheme, but the study focuses on routing aspects, and no specific MAC layer protocol is considered. Other studies aimed at computing energy consumption in WSNs that use an SDC-based MAC have also considered an APT scheme and even some degree of heterogeneity among SNs [19,20]. However, these studies have been accomplished mainly by simulation or direct measurements on laboratory prototypes.

In [21], the authors proposed a DTMC-based model of a WSN, where SNs deploy an SDC-based MAC and an APT scheme. The study evaluates different performance parameters, including energy consumption. However, this study does not consider heterogeneous scenarios or priority assignments. Furthermore, although the energy analysis considers the different SN operation cycles and operation modes, the energy consumption methodology proposed in our current study, which is based on fully exploiting the stationary probability distribution, leads to a more systematic and accurate approach than the one proposed there.

In [22], we derived closed-form expressions to determine the energy consumed by SNs in a WSN scenario where SNs deploy the PSA-MAC protocol. The study considered the full operation cycle, including the *sync*, *data*, and *sleep* periods. However, the proposed model there supported neither heterogeneous scenarios that consider different SN classes and priorities nor an APT scheme.

The PSA-MAC protocol operating in heterogeneous scenarios was also studied and evaluated in [23]. The approach used there to determine energy consumption is similar to the one used in this current work. However, we now extend the study to scenarios where SNs deploy an APT scheme, while previously, only an SPT scheme was considered.

In [24], we extended the approach proposed in [23] to compute energy consumption to support APT schemes. However, in this previous study, only the energy consumed during the *data* period was considered. In the current study, we extend previous studies by including new components of the energy consumption that were not considered in [24].

The key differential contribution of this study, with respect to prior contributions, lies in the development of novel expressions that enable the computation of energy consumption along the entire operational cycle of SNs, taking into account the complexity and challenges that arise in heterogeneous scenarios. One of the main challenges of the current study has been the design of a methodology that allows the definition of the expressions to determine energy consumption in a systematic and conceptually simple way.

The remainder of the article is organized as follows. In Section 2, an introductory description of the heterogeneous scenarios of interest and the APT scheme is provided. We introduce the system model in Section 3. A detailed description of the newly proposed expressions to determine the energy consumption is presented in Section 4. In Section 5, the evaluation scenarios are defined, and the results of our model to determine the energy consumption are depicted. Finally, the conclusions are presented in Section 6.

Significance of the Contribution

The main contribution of this work is the analytical modeling and comprehensive assessment of the energy consumed by the SNs of a WSN that deploys the PSA-MAC protocol. In the proposed model, SNs have different loads, MAC parameters, and access priorities and may use the SPT or APT schemes.

The model is based on two two-dimensional Discrete-Time Markov Chains (2D-DTMC). We propose comprehensive closed-form expressions based solely on the stationary probability distribution of the two previous DTMCs. These expressions allow the determination of the average energy consumed by SNs in a cycle of operation in network scenarios that consider the coexistence of different SN classes, priority assignments, and all the additional above-mentioned features of the PSA-MAC protocol.

SNs deploying the PSA-MAC protocol perceive the time as partitioned into cycles, and each cycle is further divided into three parts (*periods*): *sync* (synchronization), *data* and *sleep*. In addition, the PSA-MAC protocol considers *normal* and *awake* operating cycles. In *normal* cycles, an active SN willing to transmit a packet enters the *sleep* period after transmitting a packet, either with success or failure or when it senses a busy medium before its backoff timer expires. Active SNs are those with packets to send. In *awake* cycles, SNs do not enter the *sleep* mode but stay awake, listening to the transmission of possible synchronization (SYNC) packets from neighboring SNs until the cycle ends. SYNC packets are used by SNs to update their synchronization calendar and, in this way, synchronize their cycle initiation instants.

The current traffic model is mainly based on the model presented in [23]. However, in the current study, a significant extension is proposed to compute the energy consumed by an SN along the entire operation cycle. While, in the previous model only the *data* period of a cycle was considered. Here, we also include the *sync* and *sleep* periods.

The total energy a SN consumes is computed as the summation of different terms: (i) the energy consumed during *normal* cycles; (ii) the energy consumed during *awake* cycles; (iii) the energy consumed during *data* periods; and (iv) the energy consumed during *sync* periods that occur at the beginning of each cycle. Please note that *normal* cycles repeat more frequently than *awake* cycles.

The aggregate packet transmission (APT) feature that was proposed in [24] is also integrated into the current model. However, in [24], the full operation cycle was not considered, while it is considered in the new model.

The stationary probability distribution elements are the key terms that form part of the expressions that allow the determination of the average energy consumed by SNs. In the new model, the complexity of these expressions increases as the model takes into account the energy consumed during the different periods of a cycle, as well as in *normal* and *awake* cycles.

The design of the new energy computation methodology has been quite challenging, as it must take into account the heterogeneity among SNs. A heterogeneous scenario needs to consider the multiple combinations of states in which the SNs of the network might be at each operation cycle. This highlights the importance of the contribution presented in Section 4, where expressions are defined to represent the multiple contributions that are required to determine the average energy consumed by an SN of any class along a cycle.

Finally, it is important to highlight that the methodology to compute the energy consumed by SNs proposed here is considerably more systematic than those in previously proposed approaches. Also, as shown in Section 5.5, the new energy computation methodology is very accurate.

2. Heterogeneous Scenarios and APT Transmission Scheme

Before defining the methodology used to determine the energy consumed by SNs, we briefly introduce the WSN scenario under study, the transmission schemes, the different parts that compose an operation cycle, and the operation modes of SNs. For additional details about the heterogeneous scenario, the PSA-MAC protocol operation, as well as the analytical model particularities, please refer to [23].

2.1. Network Assumptions

As a simplified example, the scenario under study is depicted in Figure 1. Two classes of SNs coexist in the WSN, C1 and C2 SNs. C1 SNs have priority over the C2 SNs for medium access. For modeling convenience, we arbitrarily select one SN from each class and refer to them as *reference nodes*, RN1 and RN2.

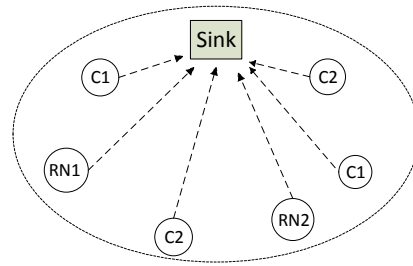


Figure 1. Heterogeneous WSN scenario with C1 and C1 SNs, and corresponding RN1 and RN2.

We focus on a single cell, where SNs are one hop away from each other. However, multiple cells together may form a larger network. SNs transmit packets towards a single destination node that we refer to as the *sink*. We assume that the *sink* node behaves as a packet absorption node, i.e., it only receives packets and never transmits them.

The network deploys the PSA-MAC protocol with the common CSMA/CA-based *RTS/CTS/DATA/ACK* packet handshake. SN that uses the PSA-MAC protocol perceive the time as partitioned into cycles, and each cycle is further divided into three parts (*periods*): *sync*, *data* and *sleep*. Also, we refer to the *active* period as the period of time composed by the aggregation of the *sync* and *data* periods. Backoff timers of active SNs that govern medium access are reset at each cycle initiation. In PSA-MAC, a SN goes to *sleep* until the next *data* period when: (i) it loses the contention (hears a busy medium before its backoff timer expires); (ii) it encounters an *RTS* collision; and (iii) after a successful transmission.

With aggregated packet transmission (APT), nodes might transmit a batch of *DATA* packets in a single cycle instead of a single one. We refer to the set of consecutive packets that will be transmitted together in the same cycle as a *packet frame* (PF). The maximum number of *DATA* packets that can be aggregated in a PF is constrained by the cycle duration T , the maximum frame length of the wireless link, by the number of *DATA* packets in the queue of the SN that gains access to the channel, and by a configurable parameter denoted by F , the maximum number of *DATA* packets that can be aggregated in a PF. SNs only transmit one PF per cycle. As an example of the operation of the AT scheme, assume that q is the number of *DATA* packets in the RN_c queue, $c = 1, 2$. When $q \leq F$, a successful PF transmission will empty its queue. However, when $q > F$, a successful PF transmission will leave $q - F$ *DATA* packets in its queue.

SNs are equipped with a battery, but energy harvesting is not supported [25]. In practical deployment scenarios, it has been shown that one or two retransmissions are sufficient to successfully send a PF [26,27]. Then, we consider an infinite retransmission model instead of the more complex finite retransmission one.

We assume that the number of *DATA* packets that arrive at the buffer of an SN follow a discrete Poisson distribution of mean λT , where λ is the *DATA* packet arrival rate and T is the cycle duration. However, the proposed analytical model is sufficiently general to accommodate any alternative discrete distribution. Each SN has a finite buffer size to hold up to Q *DATA* packets, Packets are served according to a FIFO discipline. From the MAC layer perception, we also assume that the channel is ideal (error-free).

Active SNs randomly select a backoff time with equal probability from the set $\{0, \dots, W - 1\}$, where W is the length of the contention window, measured in backoff time slots. Consider that RN_c from cluster C_c is active, $c = 1, 2$. It transmits a PF successfully (without collision) if the other contending SNs from C_c selected backoff times greater than the one chosen by the RN_c . A PF transmitted by RN_c will fail (collide) when more than one contending SN from C_c select the same backoff time as the RN_c , and the backoff time is the smallest among all contending SNs. When the backoff time generated by RN_c is not the smallest one among those generated by the other contending SNs from C_c , two outcomes are possible: (i) another SN different from RN_c can transmit successfully; (ii) other SNs different from RN_c collide while transmitting. Please note that in the latter case, RN_c will sense a busy medium before its backoff timer expires and will switch to the *sleep* mode. In

these cycles, where RN_c loses the contention, it wastes energy *overhearing* the channel. As shown later, the proposed model determines the amount of energy consumed by SNs due to *overhearing*.

2.2. Transmission and Operation Modes

Figure 2 shows the medium access procedure for both SN classes over time. Observe that C1 SNs are given medium access priority over C2 SNs, by guaranteeing that C1 SNs complete their medium access procedure before C2 SNs do it. As the proposed methodology to determine the energy consumption takes into account the energy consumed during the *sync* period, the *sync* period for both SN classes is also shown in Figure 2.

The operation of an SN almost repeats every cycle and can be summarized as progressing along the following steps. First, SNs determine a *sleep-wake up* schedule during the *sync* period. To this end, SNs exchange SYNC packets among their neighbors. The next cycle initiation instant and the corresponding SN address are included in SYNC packets. SNs use this information to synchronize their *wake up* instants at the beginning of each *sync* period. Observe from Figure 2 that both SN classes deploy the same *sync* period.

Second, during the *data* period, the conventional CSMA/CA contention scheme is used to transmit PFs. Active nodes generate a random backoff time and perform common carrier sensing. If at backoff timer expiration, a SN senses an idle channel, it sends a PF using the RTS/CTS/DATA/ACK packet handshake. A PF is recognized as successfully transmitted when the SN receives an ACK from the *sink*.

Also, the energy consumed during the *sleep* period is taken into account. As mentioned above, during this period, nodes fall asleep to save energy or remain awake to listen to SYNC packets transmitted by other SNs.

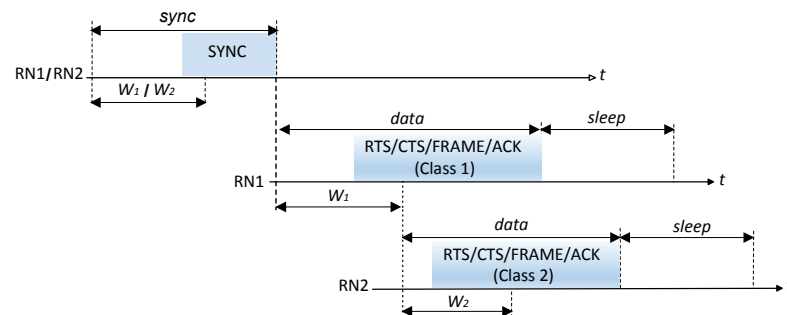


Figure 2. Transmission process in a transmission cycle for a heterogeneous WSN with two classes of nodes.

Prioritization Scheme

As C1 SNs have access priority over C2 SNs, the *data* period is initiated and completed by active C1 SNs first, if any. Active C2 SNs *wake up* shortly after C1 contention window (W_1) ends, and if they find an idle medium, C2 SNs initiate their medium access contention. However, if active C2 SNs sense a busy medium, they return to *sleep* mode and *wake up* again at the next cycle. We assume that the transmission time of the shortest C1 PF (one DATA packet) exceeds W_1 .

Please note that we assume that the energy consumed by C2 SNs to sense a busy medium takes a single backoff time slot and, therefore, it is negligible. Note also that when C1 SNs collide, C2 SNs will also detect a busy medium, and they will refrain from contending in this cycle.

3. System Model

The system model that has been developed to evaluate the WSN performance was presented in [23,24]. The model considers a pair of coupled 2D-DTMCs, whose solution in terms of their stationary probability distributions is used to derive expressions that allow to compute of the energy consumption.

3.1. Medium Access

We denote by N_1 and N_2 the total number of SNs in each class. Let us assume that RN_c , $c = 1, 2$, is active in a given cycle, and let k denote the number of C_c SNs, different from RN_c , that are also active in the same cycle, $0 \leq k \leq N_c - 1$. We denote by $P_{s,k,c}$, $P_{f,k,c}$, and $P_{sf,k,c}$, the probabilities that RN_c transmits a PF successfully, with failure (collision), or just transmits a PF either with success or failure, respectively, when contending with other k C_c SNs. Also, we denote by $BT_{s,k,c}$, and $BT_{f,k,c}$ the average backoff times generated by RN_c , conditioned on it transmits a PF with success or failure (collision), respectively, when contending with other k C_c SNs. Please refer to [23] for details on how these parameters are determined.

3.2. Definition of the 2D-DTMCs

We propose a single 2D-DTMC per SN class to model the evolution of the state of nodes (active or inactive) and their queue lengths over time. More specifically, let (i, m) be the state of an SN class, where i denotes the number of *DATA* packets in the corresponding RN queue, $0 \leq i \leq Q$, and m denotes the number of active nodes of the class, different from the RN, ($m < N - 1$). Let $P_{(i,m),(j,n)}$ denote the transition probability from state (i, m) to state (j, n) .

It is important to highlight that transition probabilities for each DTMC are substantially different from the ones defined in [23], as now they must take into account the fact that SNs might transmit multiple *DATA* packets (a PF) in a single cycle. For convenience, these new transition probabilities are defined in [28]. Please refer to this document for a detailed description of their definition.

We denote by $R_{1,0}$ the fraction of cycles in which all C_1 SNs are inactive and, therefore, there would be no PF transmissions from C_1 SNs. Clearly, $R_{1,0}$ is the fraction of cycles in which active C_2 SNs can contend for medium access. $R_{1,0}$ is the key coupling mechanism between the pair of DTMCs. The DTMC associated with C_1 SNs is independent from the one associated with C_2 SNs. Therefore, once the DTMC for C_1 is solved, $R_{1,0}$ can be determined and then, C_2 DTMC can be solved.

3.3. Solution of the 2D-DTMCs

Let $\pi_c(i, m)$ be the stationary probability of finding C_c SNs in state (i, m) . That is, the fraction of cycles where C_c SNs are in state (i, m) . Let $\pi_c = [\pi_c(i, m)]$ be the stationary probability distribution. It can be obtained by iteratively solving the set of linear equations,

$$\pi_c = \pi_c P_c, \quad \pi_c e = \mathbf{1}, \quad (1)$$

where $P_c = [P_{c,(i,m),(j,n)}]$ is the transition probability matrix of C_c , and e is a single column matrix of ones. Please note that transition probability matrices associated with C_1 and C_2 SNs, P_1 and P_2 , respectively, contain different elements. This leads to different stationary probability distributions, π_1 and π_2 , respectively. Please refer to [28] for a detailed description of the elements of P_c and the iterative solution algorithm. Note that the elements of P_2 are dependent on $R_{1,0}$.

4. Energy Consumption

In this section, we derive expressions to determine the average energy consumed by an RN per cycle, considering the different periods in which a cycle is divided as defined in Section 2.

We define an *update supercycle* as a set of N_{sc} consecutive cycles. For simplicity, we assume that Cc SNs transmit one SYNC packet every $N_{sc,c}$ cycles $c = 1, 2$, i.e., one SYNC packet per *update supercycle*. Also, they might receive one SYNC packet per cycle in the remaining $N_{sc,c} - 1$ cycles. To avoid missing SYNC packets from neighboring nodes, occasionally, an SN keeps *awake* for a whole cycle. As these cycles are different from the *normal* cycles, which include a *sleep* period after an *active* period, we refer to them as *awake* cycles.

We define a *hypercycle* as a set of N_{aw} consecutive *update supercycles*, i.e., $N_{aw} \cdot N_{sc}$ consecutive cycles. We also assume that a Cc SN follows *awake* cycles during a complete *supercycle* ($N_{sc,c}$ consecutive cycles), whereas it follows *normal* cycles during the other $N_{aw,c} - 1$ *update supercycles* of the *hypercycle*. Clearly, these definitions of the *normal* and *awake* cycles have an impact on the energy consumed by an SN.

Only the energy consumed by the radio transceiver of an SN is considered by the model. The energy consumed due to the specific sensing tasks of SNs, being application-specific, has not been taken into account.

Along the next Sections we determine the energy consumed by RN1 and RN2. The energy consumed by any other node of the same class is the same as the one consumed by the corresponding RN.

4.1. Average Energy Consumed by RNc in the Sync Period

During the *sync* period, SNs exchange SYNC packets to synchronize their *sleep-wake up* schedules. The duration of the *sync* period for Cc SNs can be determined as, $T_{sc,c} = (W_c - 1) + t_{SYNC} + D_p$, where W_c is the length of the contention window for Cc SNs, t_{SYNC} is the transmission time of a SYNC packet, and D_p is the one-way propagation delay.

The average energy consumed by a Cc SN during a *sync* period, $E_{sc,c}$, can be determined as,

$$E_{sc,c} = \frac{1}{N_{sc,c}} \cdot [(t_{SYNC} \cdot P_{tx,c} + (T_{sync,c} - t_{SYNC}) \cdot P_{rx,c})] + \frac{N_{sc} - 1}{N_{sc}} \cdot (T_{sync,c} \cdot P_{rx,c}), \quad (2)$$

where $P_{tx,c}$ and $P_{rx,c}$ are the transmission and reception power levels for Cc SNs, respectively.

4.2. Average Energy Consumed by RN1 in the Data Period

The average energy consumed by RN1 while being active in a *data* period is composed of different terms, each of which depends on the possible outcomes of the contention process: (i) it completes a successful PF transmission, $E_{tx,s}^{d,1}$; (ii) a PF transmitted by RN1 collides, $E_{tx,f}^{d,1}$; (iii) one or more C1 SNs, different from RN1, win the contention and transmit a PF, $E_{oh}^{d,1}$. In the last case, the RN1 will sense a busy channel before its backoff timer expires, and it will switch to the *sleep* mode. However, it has been listening to the channel (*overhearing*) until detecting it was busy, and this wasted energy consumption must be taken into account.

$$\begin{aligned} E_{tx,s}^{d,1} &= \sum_{i=1}^{Q_1} \sum_{k=0}^{M_1} \pi_1(i, k) P_{s,k,1} \left(E_1^{d,1} + B T_{s,k,1} P_{rx,1} + \alpha_1 t_{DATA} P_{tx,1} \right), \\ E_1^{d,1} &= t_{RTS} P_{tx,1} + [t_{CTS} + t_{ACK} + 4D_p] P_{rx,1}, \\ \alpha_1 &= \min(i, F_1). \end{aligned} \quad (3)$$

where Q_1 is RN1 buffer size in *DATA* packets, $M_1 = N_1 - 1$ is the number of C1 SNs different from RN1, α_1 is the number of *DATA* packets aggregated in the current PF, F_1 is the maximum number of *DATA* packets that C1 SNs can aggregate, t_{RTS} , t_{DATA} , t_{CTS} , and

t_{ACK} are the transmission times of the corresponding packets, and $P_{s,k,1}$ and $BT_{s,k,1}$ were already defined in Section 3.1.

$$E_{tx,f}^{d,1} = \sum_{i=1}^{Q_1} \sum_{k=0}^{M_1} \pi_1(i,k) P_{f,k,1} (E_2^{d,1} + BT_{f,k,1} P_{rx,1}), \quad (4)$$

$$E_2^{d,1} = t_{RTS} P_{tx,1} + 2D_p P_{rx,1}.$$

$$E_{oh}^{d,1} = \sum_{i=1}^{Q_1} \sum_{k=1}^{M_1} \pi_1(i,k) k P_{s,k,1} [BT_{s,k,1} + t_{RTS}] P_{rx,1} \\ + \sum_{i=1}^{Q_1} \sum_{k=2}^{M_1} \pi_1(i,k) \hat{P}_{f,k,1} BT_{f,k,1} P_{rx,1}, \quad (5)$$

$$\hat{P}_{f,k,1} = \sum_{i=1}^{W_1} \left[\sum_{n=2}^k \binom{k}{n} \left(\frac{1}{W_1} \right)^n \left(\frac{W_1 - i}{W_1} \right)^{k-n+1} \right].$$

where $\hat{P}_{f,k,1}$ is the probability that PFs transmitted by other SNs different from RN1 collide, in a cycle where RN1 is active but loses the contention, and $P_{f,k,1}$ and $BT_{f,k,1}$ were already defined in Section 3.1.

The average energy consumed by RN1 along the *data* period of a cycle can be determined as

$$E_{d,1} = E_{tx,s}^{d,1} + E_{tx,f}^{d,1} + E_{oh}^{d,1}. \quad (6)$$

4.3. Average Energy Consumed by RN2 in the Data Period

For RN2, the average energy it consumes along the *data* period of a cycle can be expressed as,

$$E_{d,2} = (E_{tx,s}^{d,2} + E_{tx,f}^{d,2} + E_{oh}^{d,2}) R_{1,0}. \quad (7)$$

where $E_{tx,s}^{d,2}$, $E_{tx,f}^{d,2}$ and $E_{oh}^{d,2}$ have the same terms as those shown in (3)–(5), but appropriately adapted for the specific features of C2 SNs.

4.4. Average Energy Consumed by RN1 during Awake Cycles

When RN1 is in *awake* mode, it wakes up at the beginning of *awake* cycles and remains awake until the cycle ends. During *awake* cycles, RN1 listens to the channel for the possible transmission of SYNC packets from neighboring SNs. For energy conservation, when RN1 hears a RTS packet, indicating the beginning of a PF transmission, it calculates the time the channel will remain occupied from the information contained in the RTS packet, and switches to the *sleep* mode. When the PF transmission ends, it returns to the *awake* state.

We now determine the average energy consumed by RN1 per *awake* cycle. It is assumed that SNs activate the *awake* mode at the beginning of the *data* period, i.e., once the *sync* period ends. For the average energy consumed by RN1 per *awake* cycle, we consider two terms: (i) the energy consumed due to the channel listening activity; (ii) the energy consumed due to being in the *sleep* mode while other SNs occupy the channel.

We consider the following cycle types:

Cycle 1A: RN1 is active, ($i_1 > 0, k_1 \geq 0$).

Zero or more C1 SNs might also be active. When other SNs are active, in addition to RN1, the following contention outcomes are possible: (i) RN1 completes a successful PF transmission; (ii) the PF from RN1 collides; (iii) another node completes a successful PF transmission, and (iv) other nodes different from RN1 collide.

Cycle 1B: RN1 is inactive, ($i_1 = 0, k_1 > 0$).

C1 SNs access the channel while RN1 is *awake*. RN1 listens to the channel to decode the *RTS* packet and determine the duration of the PF transmission. The following contention outcomes are possible: (i) a SN completes a successful PF transmission; (ii) multiple PFs collide.

Cycle 1C: All C1 SNs remain inactive, including RN1, ($i_1 = 0, k_1 = 0$).

There are active C2 SNs that access the channel while RN1 is *awake*, ($i_2 > 0, k_2 > 0$). RN1 listens to the channel, decodes the *RTS* packets in collision-free cycles and determines the duration of the PF transmissions. The following contention outcomes for C2 SNs might be possible: (i) a C2 SN completes a successful PF transmission; (ii) multiple PFs from different C2 SNs collide.

Cycle 1D: All C1 and C2 SNs remain inactive, $i_1 = k_1 = i_2 = k_2 = 0$, while RN1 is *awake*.

4.4.1. Average Energy Consumed by RN1 in Type 1A Cycles

Let $E_{tx,s}^{aw}[1A]$, $E_{tx,f}^{aw}[1A]$ and $E_{oh}^{aw}[1A]$ be the average energy consumed by RN1 in type 2A cycles when RN1 completes a successful PF transmission, a PF from RN1 collides, and RN1 overhears PF transmissions from other C1 SNs, respectively.

These RN1 energy consumption terms can be determined as,

$$E_{tx,s}^{aw}[1A] = \sum_{i=1}^{Q_1} \sum_{k=1}^{M_1} \pi_1(i, k) P_{s,k,1} \left[E_1^{aw,1} - (BT_{s,k,1} + \alpha_1 t_{DATA}) P_{rx,1} \right], \quad (8)$$

$$E_1^{aw,1} = [T - T_{sc,1} - (t_{RTS} + t_{CTS} + t_{ACK} + 4D_p)] P_{rx,1}.$$

$$E_{tx,f}^{aw}[1A] = \sum_{i=1}^{Q_1} \sum_{k=1}^{M_1} \pi_1(i, k) P_{f,k,1} \left[E_2^{aw,1} - BT_{f,k,1} P_{rx,1} \right], \quad (9)$$

$$E_2^{aw,1} = [T - T_{sc,1} - (t_{RTS} + 2D_p)] P_{rx,1}.$$

$$E_{oh}^{aw}[1A] = \sum_{i=1}^{Q_1} \sum_{k=1}^{M_1} \pi_1(i, k) k P_{s,k,1} \left[E_3^{aw,1} - \hat{f}_{k,1} t_{DATA} (P_{rx,1} - P_{sl}) \right]$$

$$+ \sum_{i=1}^{Q_1} \sum_{k=2}^{M_1} \pi_1(i, k) \hat{P}_{f,k,1} (T - T_{sc,1}) P_{rx,1},$$

$$E_3^{aw,1} = (T - T_{sc,1}) P_{rx,1} - (t_{CTS} + t_{ACK} + 3D_p) (P_{rx,1} - P_{sl}), \quad (10)$$

$$\hat{P}_{f,k,1} = \sum_{i=1}^{W_1} \left[\sum_{n=2}^k \binom{k}{n} \left(\frac{1}{W_1} \right)^n \left(\frac{W_1 - i}{W_1} \right)^{k-n+1} \right],$$

$$\hat{f}_{k,1} = \frac{1}{G_{k,1}} \sum_{i=1}^{Q_1} \alpha_1 \cdot \pi_1(i, k), \quad G_{k,1} = \sum_{i=1}^{Q_1} \pi_1(i, k).$$

where T is the cycle duration, $\hat{P}_{f,k,1}$ is the probability that PFs transmitted by other SNs, different from RN1, collide in cycles where RN1 is active but loses the contention, $\hat{f}_{k,1}$ is the average PF size transmitted by C1 SNs, conditioned on RN1 being contending with other k C1 SNs in the same cycle, and P_{sl} is the power level in *sleep* mode [23]. Please note that $\hat{f}_{k,1}$ is obtained to determine the average time that RN1 will remain in the *sleep* mode awaiting the end of the PF transmission. Note also that $\hat{f}_{k,1} = 1$ when the SPT scheme is deployed.

Then, the average energy consumed by RN1 in type 1A *awake* cycles is

$$E_{aw}[1A] = E_{tx,s}^{aw}[1A] + E_{tx,f}^{aw}[1A] + E_{oh}^{aw}[1A]. \quad (11)$$

4.4.2. Average Energy Consumed by RN1 in Type 1B Cycles

The average energy consumed by RN1 in type 1B *awake* cycles can be determined as

$$\begin{aligned}
 E_{aw}[1B] &= \sum_{k=1}^{M_1} \pi_1(0, k) k P_{s, k-1, 1} \left[E_3^{aw, 1} - \hat{f}_{k-1, 1} t_{DATA} (P_{rx, 1} - P_{sl}) \right] \\
 &\quad + \sum_{k=2}^{M_1} \pi_1(0, k) \hat{P}'_{f, k, 1} (T - T_{sc, 1}) P_{rx, 1}, \\
 \hat{P}'_{f, k, 1} &= \sum_{i=1}^{W_1} \left[\sum_{n=2}^k \binom{k}{n} \left(\frac{1}{W_1} \right)^n \left(\frac{W_1 - i}{W_1} \right)^{k-n} \right],
 \end{aligned} \tag{12}$$

where $\hat{P}'_{f, k, 1}$ denotes the probability that two or more of the k SNs, other than RN1, transmit with collision while RN1 is inactive. Please note that $\hat{f}_{k-1, 1}$ can be obtained as in (10).

4.4.3. Energy Consumption in Type 1C Cycles

The energy consumed by RN1 in type 1C *awake* cycles can be determined as

$$\begin{aligned}
 E_{aw}[1C] &= \sum_{i=1}^{Q_2} \sum_{k=1}^{M_2} \pi_2(i, k) (k + 1) P_{s, k, 2} \left[E_3^{aw, 1} - \hat{f}_{k, 2} t_{DATA} (P_{rx, 1} - P_{sl}) \right] \\
 &\quad + \sum_{k=1}^{M_2} \pi_2(0, k) k P_{s, k-1, 2} \left[E_3^{aw, 1} - \hat{f}_{k-1, 2} t_{DATA} (P_{rx, 1} - P_{sl}) \right] \\
 &\quad + \sum_{i=1}^{Q_2} \sum_{k=2}^{M_2} \pi_2(i, k) \hat{P}_{f, k, 2} (T - T_{sc, 1c}) P_{rx, 1} \\
 &\quad + \sum_{k=2}^{M_2} \pi_2(0, k) \hat{P}'_{f, k, 2} (T - T_{sc, 1}) P_{rx, 1}, \\
 \hat{f}_{k, 2} &= \frac{1}{G_{k, 2}} \sum_{i=1}^{Q_2} \alpha_1 \cdot \pi_2(i, k), \quad G_{k, 2} = \sum_{i=1}^{Q_2} \pi_2(i, k).
 \end{aligned} \tag{13}$$

where $\hat{P}_{f, k, 2}$ is the probability that PFs transmitted by RN2 collide while contending with other additional k C2 SNs, $\hat{P}'_{f, k, 2}$ is the probability that two or more of the k active SNs, other than RN2, transmit with collision while RN2 is inactive, $\hat{f}_{k, 2}$ is the average PF size transmitted by RN2, conditioned on RN2 being contending with other k C2 SNs in the same cycle, $\alpha_2 = \min(i, F_2)$ is the number of *DATA* packets aggregated in the current PF, F_1 is the maximum number of *DATA* packets that C2 SNs can aggregate, $\hat{P}_{f, k, 2}$, $\hat{P}'_{f, k, 2}$, $\hat{f}_{k, 2}$ and $\hat{f}_{k-1, 2}$ can be determined in the same way as their C1 counterparts.

As before, note that $\hat{f}_{k, 2}$ $\hat{f}_{k-1, 2}$ are obtained to determine the average time RN1 will remain in the *sleep* mode while waiting for the end of the PF transmitted by a C2 SNs. Note also that $\hat{f}_{k, 2} = 1$ when the SPT scheme is deployed.

Each of the terms in expression (13) defines the average energy consumed by RN1 due to the occurrence of different events. The first term accounts for the average energy consumed when one of the $k + 1$ active C2 SNs (the RN2 and other k C2 SNs) transmits a PF successfully. The second term accounts for the average energy consumed when one of the k active C2 SNs other than RN2, transmits a PF successfully in a cycle where RN2 is inactive. The third and fourth account for the average energy consumed when two or more of k C2 SNs, different from the RN2, transmit with collision when the RN2 is active or inactive, respectively.

4.4.4. Energy Consumption in in Type 1D Cycles

The average energy consumed by RN1 in type 1D *awake* cycles can be determined as

$$E_{aw}[1D] = \pi_1(0,0)\pi_2(0,0)(T - T_{sc,1})P_{rx,1}. \quad (14)$$

4.4.5. Average Energy Consumed by RN1 in *awake* Cycles

The total average energy consumed by RN1 in *awake* cycles can be determined as

$$\begin{aligned} E_{aw,1} &= E_{aw}[1A] + E_{aw}[1B] + R_{1,0}E_{aw}[1C] + E_{aw}[1D], \\ E_{aw,1} &= E_{tx,s}^{aw}[1A] + E_{tx,f}^{aw}[1A] + E_{oh}^{aw}[1A] + E_{aw}[1B] + R_{1,0}E_{aw}[1C] + E_{aw}[1D]. \end{aligned} \quad (15)$$

Please note that $E_{aw}[1C]$ is weighted by the fraction of cycles where C1 SNs remain inactive, $R_{1,0}$. In these cycles, active C2 SNs, if any, will contend for medium access.

4.5. Average Energy Consumed by RN2 during *Awake* Cycles

As the operation of RN1 and RN2 during *awake* cycles is similar, please refer to Section 4.4 for the operational specific details. We now determine the average energy consumed by RN2 per *awake* cycle. We consider two terms: (i) the energy consumed due to the channel listening activity; (ii) the energy consumed due to being in the *sleep* mode while other SNs occupy the channel.

We identify the following cycle types:

Cycle 2A: C1 SNs are inactive ($i_1 = 0, k_1 = 0$), but RN2 and other C2 SNs are active ($i_2 > 0, k_2 \geq 0$). Either RN2 or any other active C2 SNs will access the channel, while RN2 is awake in the same cycle. The possible contention outcomes are: (a) RN2 successfully transmits a PF; (b) a PF transmitted by RN2 collides; (c) another C2 SN successfully transmits a PF; (d) other C2 SNs collide.

Cycle 2B: C1 SNs are inactive, RN2 is also inactive, but other C2 SNs are active, ($i_2 = 0, k_2 > 0$). C2 SNs access the channel in the same cycle that RN2 is awake. The possible contention outcomes are: (a) a C2 SN successfully transmits a PF; (b) multiple C2 SNs collide.

Cycle 2C: All C1 SNs are active, ($i_1 \geq 0, k_1 \geq 0$), while C2 SNs, including RN1 SNs, are inactive, ($i_2 = 0, k_2 = 0$). The possible contention outcomes are: (a) a C1 SN successfully transmits a PF; (b) multiple C1 SNs collide.

Cycle 2D: RN2 and the rest of C1 and C2 SNs are inactive, $i_1 = k_1 = i_2 = k_2 = 0$. Please note that in cycles of type 2D, both RN1 and RN2 might simultaneously coincide in their respective *awake* cycles.

4.5.1. Energy Consumption in Type 2A Cycles

Let $E_{tx,s}^{aw}[2A]$, $E_{tx,f}^{aw}[2A]$ and $E_{oh}^{aw}[2A]$, be the average energy consumed by RN2 in type 1A cycles when RN2 completes a successful PF transmission, a PF from RN2 collides, and RN2 *overhears* a PF transmission from other C2 SNs, respectively.

These RN2 energy consumption terms can be determined as,

$$\begin{aligned} E_{tx,s}^{aw}[2A] &= \sum_{i=1}^{Q_2} \sum_{k=1}^{N_2} \pi_2(i,k)P_{s,k,2} \left[E_1^{aw,2} - (\alpha_2 t_{DATA} + BT_{s,k,2})P_{rx,2} \right], \\ E_1^{aw,2} &= [T - T_{sc,2} - (t_{RTS} + t_{CTS} + t_{ACK} + 4D_p)]P_{rx,2}, \\ \alpha_2 &= \min(i, F_2). \end{aligned} \quad (16)$$

$$\begin{aligned} E_{tx,f}^{aw}[2A] &= \sum_{i=1}^{Q_2} \sum_{k=1}^{N_2} \pi_2(i,k)P_{f,k,2} \left[E_2^{aw,2} - BT_{f,k,2}P_{rx,2} \right], \\ E_2^{aw,2} &= [T - T_{sc,2} - (t_{RTS} + 2D_p)]P_{rx,2}. \end{aligned} \quad (17)$$

$$\begin{aligned}
E_{oh}^{aw}[2A] &= \sum_{i=1}^{Q_2} \sum_{k=1}^{N_2} \pi_2(i, k) k P_{s,k,2} \left[E_3^{aw,2} - \hat{f}_{k,2} t_{DATA} (P_{rx,2} - P_{sl}) \right] \\
&+ \sum_{i=1}^{Q_2} \sum_{k=2}^{N_2} \pi_2(i, k) \hat{P}_{f,k,2} (T - T_{sc,2}) P_{rx,2}, \\
E_3^{aw,2} &= (T - T_{sc,2}) P_{rx,2} - (t_{CTS} + t_{ACK} + 3D_p) (P_{rx,2} - P_{sl}).
\end{aligned} \tag{18}$$

where α_2 , F_2 , $\hat{P}_{f,k,2}$ and $\hat{f}_{k,2}$ have identical meaning and purpose than their C1 counterparts defined in (10).

Then, the average energy consumed by RN2 in type 1A *awake* cycles is,

$$E_{aw}[2A] = E_{tx,s}^{aw}[2A] + E_{tx,f}^{aw}[2A] + E_{oh}^{aw}[2A]. \tag{19}$$

4.5.2. Energy Consumption in Type 2B Cycles

The average energy consumed by RN2 in type 2B *awake* cycles can be determined as

$$\begin{aligned}
E_{aw}[2B] &= \sum_{k=1}^{N_2} \pi_2(0, k) k P_{s,k-1,2} \left[E_3^{aw,2} - \hat{f}_{k-1,2} t_{DATA} (P_{rx,2} - P_{sl}) \right] \\
&+ \sum_{k=2}^{N_2} \pi_2(0, k) \hat{P}'_{f,k,2} (T - T_{sc,2}) P_{rx,2}.
\end{aligned} \tag{20}$$

where, as for C1 SNs, $\hat{P}'_{f,k,2}$ is the probability that one of the k C2 SNs, different from RN2, transmits a PF with collision when RN2 is inactive.

4.5.3. Energy Consumption in Type 2C Cycles

The average energy consumed by RN2 in type 2C *awake* cycles can be determined as

$$\begin{aligned}
E_{aw}[2C] &= \sum_{i=1}^{Q_1} \sum_{k=1}^{N_1} \pi_1(i, k) (k+1) P_{s,k,1} \left[E_3^{aw,2} - \hat{f}_{k,1} t_{DATA} (P_{rx,2} - P_{sl}) \right] \\
&+ \sum_{k=1}^{N_1} \pi_1(0, k) k P_{s,k-1,1} \left[E_3^{aw,2} - \hat{f}_{k-1,1} t_{DATA} (P_{rx,2} - P_{sl}) \right] \\
&+ \sum_{i=1}^{Q_1} \sum_{k=2}^{N_1} \pi_1(i, k) \hat{P}_{f,k,1} (T - T_{sc,2}) P_{rx,2} \\
&+ \sum_{k=2}^{N_1} \pi_1(0, k) \hat{P}'_{f,k,1} (T - T_{sc,2}) P_{rx,2}.
\end{aligned} \tag{21}$$

The type of events associated with the different terms in the expression above have the same meaning and purpose as their C1 counterparts, that were described in Section 4.4.3.

4.5.4. Energy Consumption in Type 2D Cycles

The average energy consumed by RN2 in type 2D *awake* cycles can be determined as

$$E_{aw}[2D] = \pi_1(0, 0) \pi_2(0, 0) (T - T_{sc,2}) P_{rx,2}. \tag{22}$$

4.5.5. Average Energy Consumed by RN2 in *Awake* Cycles

The total average energy consumed by RN2 in *awake* cycles can be determined as

$$\begin{aligned}
E_{aw,2} &= (E_{aw}[2A] + E_{aw}[2B]) R_{1,0} + E_{aw}[2C] + E_{aw}[2D], \\
E_{aw,2} &= \left(E_{tx,s}^{aw}[2A] + E_{tx,f}^{aw}[2A] + E_{oh}^{aw}[2A] + E_{aw}[2B] \right) R_{1,0} \\
&+ E_{aw}[2C] + E_{aw}[2D].
\end{aligned} \tag{23}$$

Observe that $E_{aw}[2A]$ and $E_{aw}[2B]$ are weighted by $R_{1,0}$, the fraction of cycles where C1 SNs are inactive.

4.6. Average Energy Consumption during Normal Cycles

Recall that after a successful or failed PF transmission, SNs switch to the *sleep* mode during the rest of the cycle to save energy. We refer to these cycles as *normal* cycles. In this subsection, we determine the average energy consumed by an RN in a *normal* cycle exclusively due to being in the *sleep* mode.

4.6.1. C1 Sensor Nodes

The average energy consumed by RN1 in a *normal* cycle can be expressed as being composed of different terms, each of them depends on the possible outcomes of the RN1 contention process: (i) it completes a successful PF transmission, $E_{tx,s}^{nr,1}$; (ii) a PF transmitted by RN1 collides, $E_{tx,f}^{nr,1}$; (iii) one or more C1 SNs, different from RN1, win the contention and transmit a PF, $E_{oh}^{nr,1}$.

$$E_{tx,s}^{nr,1} = \sum_{i=1}^{Q_1} \sum_{k=0}^{M_1} \pi_1(i,k) P_{s,k,1} T_1^{nr,1} P_{sl},$$

$$T_1^{nr,1} = T - T_{sc,1} - (BT_{s,k,1} + t_{RTS} + \alpha_1 t_{DATA} + t_{CTS} + t_{ACK} + 4D_p),$$

$$\alpha_1 = \min(i, F_1).$$
(24)

$$E_{tx,f}^{nr,1} = \sum_{i=1}^{Q_1} \sum_{k=1}^{M_1} \pi_1(i,k) P_{f,k,1} T_2^{nr,1} P_{sl},$$

$$T_2^{nr,1} = T - T_{sc,1} - (BT_{f,k,1} + t_{RTS} + D_p).$$
(25)

$$E_{oh}^{nr,1} = \sum_{i=1}^{Q_1} \sum_{k=1}^{M_1} \pi_1(i,k) P_{s,k,1} (T_3^{nr,1} - BT_{s,k,1}) P_{sl}$$

$$+ \sum_{i=1}^{Q_1} \sum_{k=2}^{M_1} \pi_1(i,k) \hat{P}_{f,k,1} (T_3^{nr,1} - BT_{f,k,1}) P_{sl}$$

$$+ \sum_{k=0}^{M_1} \pi_1(0,k) (T - T_{sc,1}) P_{sl},$$

$$T_3^{nr,1} = T - T_{sc,1} - (t_{RTS} + D_p).$$
(26)

The average energy consumed by RN1 in a *normal* cycles can be expressed as,

$$E_{nr,1} = E_{tx,s}^{nr,1} + E_{tx,f}^{nr,1} + E_{oh}^{nr,1}.$$
(27)

4.6.2. C2 Sensor Nodes

The average energy consumed by RN2 in a *normal* cycle can be expressed as being composed of different terms, each of them associated with the occurrence of the possible outcomes of the RN2 contention process. RN2 switches to *sleep* mode when any of the following events occur: (i) RN2 completes the transmission of a PF with success, $E_{tx,s}^{nr,2}$; (ii) RN2 detects a collision when transmitting a PF, $E_{tx,f}^{nr,2}$; (iii) an active RN2 detects that it has lost the contention with other C2 SNs, $E_{oh}^{nr,2}$; (iv) in cycles in which all C2 are inactive, $E_{id}^{nr,2}$. (v) along any cycles in which C1 SNs access the channel and, therefore, the medium is busy for C2 SNs, $E_{bm}^{nr,2}$;

$$\begin{aligned}
E_{tx,s}^{nr,2} &= \sum_{i=1}^{Q_2} \sum_{k=0}^{M_2} \pi_2(i,k) P_{s,k,2} \left[T_1^{nr,2} - (BT_{s,k,2} + \alpha_2 t_{DATA}) \right] P_{sl} R_{1,0}, \\
T_1^{nr,2} &= T - T_{sc,2} - (t_{RTS} + t_{CTS} + t_{ACK} + 4D_p), \\
\alpha_2 &= \min(i, F_2).
\end{aligned} \tag{28}$$

$$\begin{aligned}
E_{tx,f}^{nr,2} &= \sum_{i=1}^{Q_2} \sum_{k=1}^{M_2} \pi_2(i,k) P_{f,k,2} \left[T_2^{nr} - BT_{f,k,2} \right] P_{sl} R_{1,0}, \\
T_2^{nr,2} &= T - T_{sc,2} - (t_{RTS} + 2D_p).
\end{aligned} \tag{29}$$

$$\begin{aligned}
E_{oh}^{nr,2} &= \sum_{i=1}^{Q_2} \sum_{k=1}^{M_2} \pi_2(i,k) k P_{s,k,2} \left(T_3^{nr,2} - BT_{s,k,2} \right) P_{sl} R_{1,0} \\
&\quad + \sum_{i=1}^{Q_2} \sum_{k=2}^{M_2} \pi_2(i,k) \hat{P}_{f,k,2} + \left(T_3^{nr,2} - BT_{f,k,2} \right) P_{sl} R_{1,0}, \\
T_3^{nr,2} &= T - T_{sc,2} - t_{RTS} - D_p.
\end{aligned} \tag{30}$$

$$E_{id}^{nr,2} = \sum_{k=0}^{M_2} \pi_2(0,k) (T - T_{sc,2}) P_{sl} R_{1,0}. \tag{31}$$

$$E_{bm}^{nr,2} = (T - T_{sc,2}) P_{sl} (1 - R_{1,0}). \tag{32}$$

The average energy consumed by RN2 in *normal* cycles can be expressed as,

$$E_{nr,2} = E_{tx,s}^{nr,2} + E_{tx,f}^{nr,2} + E_{oh}^{nr,2} + E_{id}^{nr,2} + E_{bm}^{nr,2}. \tag{33}$$

4.7. Total Average Energy Consumed by an RN in a Cycle

To calculate the total average energy consumed by an SN per cycle, E_c , we take into account all previously defined energy consumption terms

$$E_c = E_{sc,c} + E_{d,c} + E_{sl,c} + E'_{aw,c}, \quad c = 1, 2, \tag{34}$$

$$E_{sl,c} = E_{nr,c} \frac{(N_{aw,c} - 1)}{N_{aw,c}}, \tag{35}$$

$$E'_{aw,c} = E_{aw,c} \frac{1}{N_{aw,c}}. \tag{36}$$

5. Numerical Results

5.1. Scenario and Parameter Configuration

For the WSN scenario under study, the value of its different configurable parameters has been defined in Table 1.

The reception and transmission power shown in Table 1 have been obtained from [29]. To obtain them, the sensor is considered to operate with a voltage source in the range [2.7, 3.3] in volts, the consumed current of the radio transceiver is 17.4 mA while transmitting at 0 dBm, and 19.7 mA in reception mode. If we assume that a sensor operates with a 3 V voltage source, the power consumed during transmission and reception modes is 52 mW and 59 mW, respectively. This approach is similar to the one used in [30], where a model of a communication system that deploys energy harvesting is proposed.

Table 1. Parameters of the scenario under study.

Cycle time (T)	60 ms	Propagation delay (D_p)	0.1 μ s
$t_{SYNC}, t_{RTS}, t_{CTS}$ and t_{ACK}	0.18 ms	Slot time (t_s)	0.1 ms
t_{DATA}	1.716 ms	Contention window (W)	128 slots
DATA packet size (S)	50 bytes	Queue size (Q)	10 packets
update supercycle (N_{sc})	20 cycles	N_{aw}	80 supercycles
Transmission power (P_{tx})	52 mW	Reception power (P_{rx})	59 mW
Sleep power consumption (P_{sl})		$P_{sl} = 3 \mu$ W	
Maximum frame size		$F = \{2, 5, 10\}$ packets	
Nodes number		Packets arrival rate (packets/s)	
$N_1 = 5, N_2 = 20$		$\lambda_1 = \{0.5\}, \lambda_2 = [0.5, 4.5]$	

5.2. Analytical Model Validation

The proposed analytical model is an approximate model whose accuracy is validated by simulation. The analytical results have been obtained by solving the two 2D-DTMCs and finding their stationary probability distributions. On the other hand, simulation results have been obtained using a customized discrete-event simulation program developed in C language. It mimics the real behavior of the WSN. That is, in each cycle: (i) packets arrive in the queue of an SN according to a given discrete probability distribution; (ii) active SNs contend for channel access. (iii) if a SN wins the contention, it transmits a PF according to the transmission scheme configured in it (SPT or APT); (iv) if a collision occurs, all active SNs of the same class will switch to the *sleep* mode until the end of the cycle. The simulation results are completely independent from those obtained by the analytical model.

The simulation results presented have been obtained as the average of measurements performed over 10^8 cycles. We have also obtained 95% confidence level intervals for the performance parameters of interest. However, being very small, they have been mostly omitted. For illustration purposes and as examples, confidence intervals have been drawn for the curves of Figures 3 and 4. In the scenario studied in these figures, both classes deploy the SPT scheme ($F_1 = F_2 = 1$), and the queue of C1 and C2 SNs can store a maximum of $Q_1 = Q_2 = 10$ DATA packets, respectively. In these figures, black lines correspond to analytical values, while simulation values are represented by their corresponding red 95% confidence level intervals.

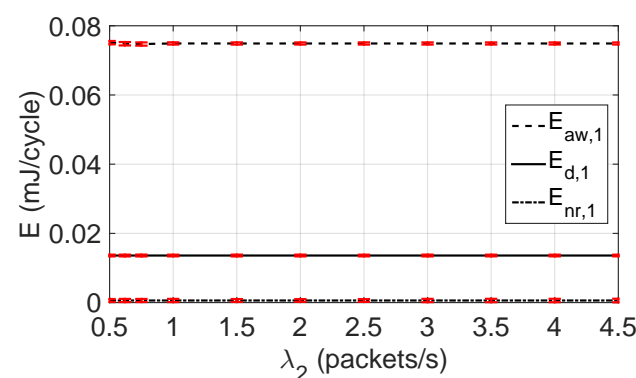


Figure 3. Average energy consumed by RN1 per cycle during the *data* period, and in the *awake* and *normal* cycles, when deploying SPT ($F_1 = 1$).

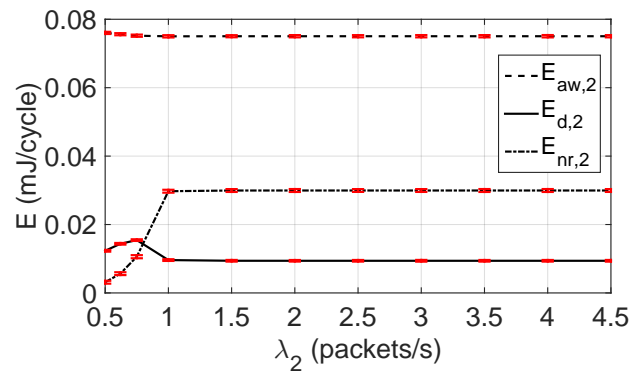


Figure 4. Average energy consumed by RN2 per cycle during the *data* period, and in the *awake* and *normal* cycles, when deploying SPT ($F_2 = 1$).

Please note that the load for C1 SNs is constant ($\lambda_1 = 0.5$ packets/s), while varies for C2 SNs. The load offered to a single C1 SN is one *DATA* packet every 33.3 cycles, approximately, for a cycle of $T = 60$ ms. The load offered to the 5 C1 SNs is 5 *DATA* packets every 33.3 cycles. On the other hand, when $\lambda_2 = 1$ packet/s, the load offered to a single C2 SN is two *DATA* packet every 33.3 cycles, approximately, and the load offered to the 20 C2 SNs is 40 *DATA* packets every 33.3 cycles.

Clearly, as λ_2 approaches 1 packet/s, the load offered to the WSN is larger than the maximum load the WSN can carry, i.e., 33.3 *DATA* packet every 33.3 cycles. As the offered load approaches the maximum carried load, the performance observed by C2 SNs degrades, as C2 SNs have lower access priority than C1 SNs. Then, as observed in Figure 4, C2 SNs experience a traffic congestion situation, even for traffic loads as small as $\lambda_2 = 0.5$ packet/s.

The energy consumed in *awake* cycles, $E_{aw,c}$, is identical for SNs of both classes. However, $E_{nr,2}$ is larger than $E_{nr,1}$. Recall that $E_{nr,c}$ measures the average energy consumed by RN c while it is in the *sleep* mode in *normal* cycles. Please note that C2 SNs experience much more frequent collisions than C1 SNs. Typically, an SN detects a collision when a *CTS* packet is not received after the transmission of the *RTS* packet. Upon detecting a collision, an SN switches to the *sleep* mode. Then, the time spent in the *sleep* mode is larger for classes that experience traffic congestion than for classes that do not experience it.

For the results presented in the following subsections, analytical results are represented by black lines with markers, while simulation results are represented by red markers. As it will be observed, the analytical and simulation markers completely overlap. This indicates a perfect match between the analytical and simulation results and proves that the results obtained by the approximate analytical model are very accurate.

5.3. Energy Consumed by RN1 and RN2 in the Data Period, the Awake and Normal Cycles

Figures 5 and 6 show the energy consumed by RN1 and RN2 when deploying the APT transmission scheme with $F_1 = F_2 = 2$ and $Q_1 = Q_2 = 10$. Figure 5 shows that the energy consumed by RN1 is virtually the same as in Figure 3, where C1 SNs deployed the SPT scheme ($F_1 = 1$).

However, Figure 6 shows that RN2 achieves the congestion state with a larger arrival rate than in the scenario of Figure 4, approximately, at an arrival rate twice as large as the previous one. In addition, the energy consumed in the congestion state is larger than the one consumed in the scenario of Figure 4, indicating that the packet throughput in the congestion state is larger when deploying $F_2 = 2$ (APT) than when deploying $F_2 = 1$ (SPT). The deployment of APT in C2 SNs implies that more packets are sent when an SN wins the contention for medium access. This reduces the average number of active C2 SNs per cycle, and, in turn, it leads to a higher medium access success rate.

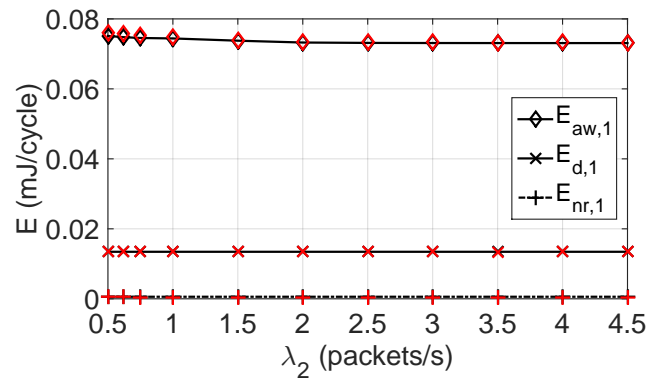


Figure 5. Average energy consumed by RN1 per cycle during the *data* period, and in the *awake* and *normal* cycles, when deploying APT ($F_1 = 2$).

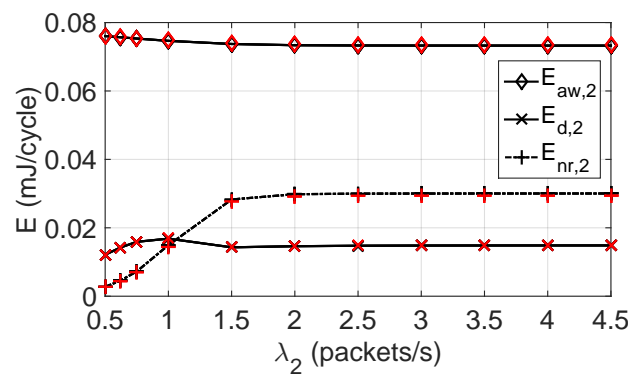


Figure 6. Average energy consumed by RN2 per cycle during the *data* period, and in the *awake* and *normal* cycles, when deploying APT ($F_2 = 2$).

Figures 7 and 8 show the energy consumed by RN1 and RN2 when deploying the APT transmission scheme with $F_1 = F_2 = 5$ and $Q_1 = Q_2 = 10$. Also, Figures 9 and 10 show the energy consumed by RN1 and RN2 when deploying the APT transmission scheme with $F_1 = F_2 = 10$ and $Q_1 = Q_2 = 10$.

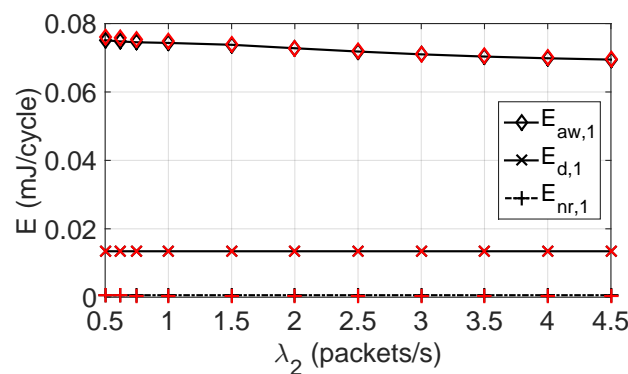


Figure 7. Average energy consumed by RN1 per cycle during the *data* period, and in the *awake* and *normal* cycles, when deploying APT ($F_1 = 5$).

As mentioned above, when large PFs are deployed ($F_c = 5, 10$), the average number of active nodes per cycle of a given class decreases with respect to scenarios with shorter PFs. This has a beneficial impact on the class, increasing its throughput and decreasing energy consumption, as fewer collisions occur and fewer retransmissions are required, which helps to conserve energy. Observe in Figure 7 that the energy consumed by C1 SNs remain almost insensitive to the increase in the maximum PF size (F_1). However, for C2

SNs, $E_{d,2}$ increases with the load, indicating that larger PFs are being transmitted when compared to the previous scenarios studied. Consequently, the C2 SNs throughput is now also higher.

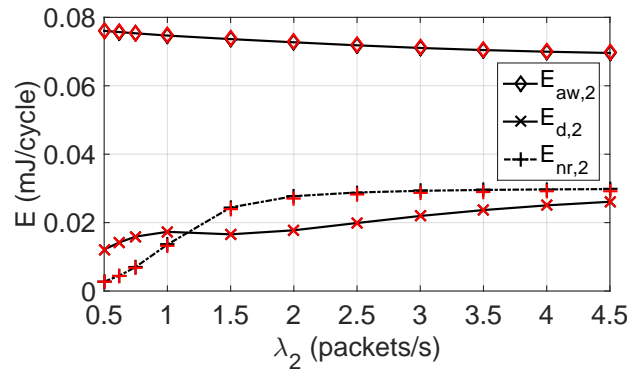


Figure 8. Average energy consumed by RN2 per cycle during the *data* period, and in the *awake* and *normal* cycles, when deploying APT ($F_2 = 5$).

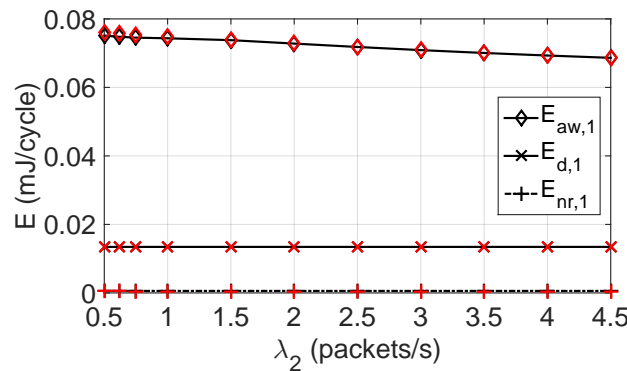


Figure 9. Average energy consumed by RN1 per cycle during the *data* period, and in the *awake* and *normal* cycles, when deploying APT ($F_1 = 10$).

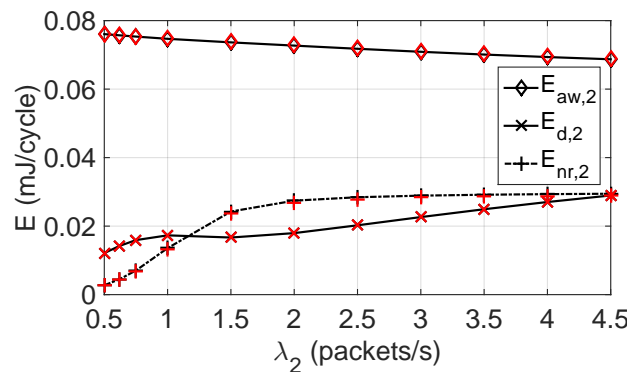


Figure 10. Average energy consumed by RN2 per cycle during the *data* period, and in the *awake* and *normal* cycles, when deploying APT ($F_2 = 10$).

Note also the trend of the energy consumed in *awake* cycles as load increases. Clearly, $E_{aw,c}$ decreases as load increases, and this trend is more pronounced as the value of F_c increases. This is because when an SN is in an *awake* cycle and transmits a PF with success, particularly when transmitting long PFs, it takes the SN longer to switch to the *awake* mode and activate the receiver. On the other hand, when an SN is in an *awake* cycle and transmits a PF that collides, the SN will switch to the *awake* operation mode and activate the receiver earlier than in cycles where the PF is successfully sent. Recall that a collision is detected quite early in the transmission process, when the corresponding CTS packet is not received.

Then, the trend of the energy consumed in *awake* cycles as load increases clearly indicates that the success rate of transmitted PF increases with load as F_c increases.

Note also that in the technical data sheet of the SN that has been used as a reference for the energy consumption values, the energy consumed in reception mode is larger than the one consumed while transmitting [29,31].

5.4. Energy Consumed by RN2 Due to PF Transmissions with Success and Failure, and Due to Overhearing

In this subsection, we present the average energy consumed by RN1 and RN2 per cycle, along the *data* period of a cycle. We represent the variation of the different components of the energy consumed with the offered load to C2 SNs (λ_2), i.e., the energy consumed due to a PF transmitted with success, $E_{tx,s}^{d,2}$, the one when a PF collides, $E_{tx,f}^{d,2}$, and the one due to RNc overhearing the transmission of PFs by other SNs of the same class that win the contention to access the medium, $E_{oh}^{d,2}$. We also represent the total average energy consumed per cycle during the *data* period of a cycle, $E_{d,2} = E_{tx,s}^{d,2} + E_{tx,f}^{d,2} + E_{oh}^{d,2}$.

We evaluate a scenario where Cc SNs deploy the APT transmission scheme with $F_1 = F_2 = 10$ and have a queue capacity of $Q_1 = Q_2 = 10$ DATA packets. The results are shown in Figure 11. Recall that $E_{oh}^{d,2}$ defines the average energy consumed by an active RN2 that loses the contention to access the channel. At the beginning of the *data* period of a cycle, active SNs start sensing the medium until their backoff timers expire or sense a busy medium. In the latter case, SNs move to the *sleep* mode until the end of the cycle. Then, $E_{oh}^{d,c}$ measures the average energy wasted by an active RNc per cycle due to having the receiver active to perform channel sensing along *data* periods where it loses the contention.

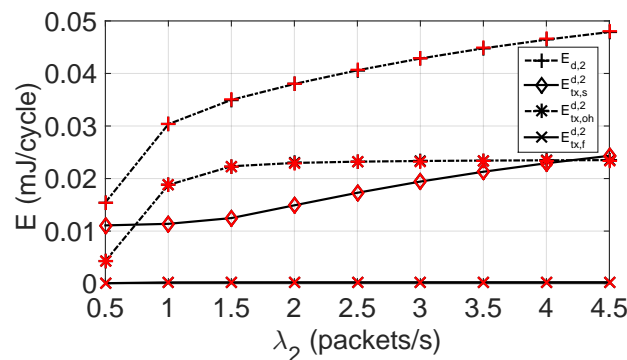


Figure 11. Average energy consumed by RN2 per cycle due to PF transmissions with success and failure, and to overhearing, when deploying APT ($F_2 = 10$).

Observe that the average energy wasted per cycle due to PF collisions, $E_{tx,f}^{d,2}$, is almost negligible. That is, when C2 SNs deploy the APT scheme with $F_2 = 10$, the packet collision rate is substantially reduced. As mentioned before, as F increases, fewer SNs per cycle are active, and a higher rate of successfully transmitted PFs is achieved.

To reinforce this perspective, we show the variation of the packet average access delay with the offered load to C2 SNs (λ_2), for different values of F in Figure 12. This figure is taken from [24]. Observe that the average DATA packet delay expressed in cycles for C1 SNs, D_1 , is insensitive to the value of F_1 . However, D_2 decreases substantially as F_2 increases, confirming the benefits that can be obtained by deploying the APT scheme.

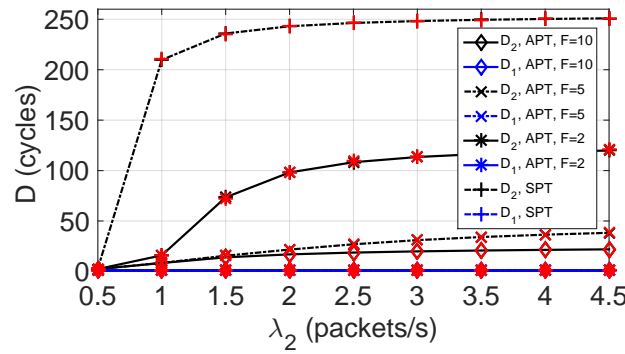


Figure 12. Average packet delay for both SNs classes.

5.5. Accuracy of the New Methodology to Determine Energy Consumption

As mentioned in Section 1, the new proposed methodology to determine the average energy consumed by an SN per cycle has proved to be more accurate and systematic than those previously proposed. In this subsection, we compare the accuracy of the new methodology and the accuracy of a previous one [23] to determine the average energy consumed by an SN per cycle in the *data* period $E_{d,c} = E_{tx,s}^{d,c} + E_{tx,f}^{d,c} + E_{oh}^{d,c}$, $c = \{1, 2\}$. Unfortunately, for the previous methodology, the average energy data consumed by an SN per cycle in the *sleep* mode and in *awake* cycles are not available.

A substantial part of the accuracy improvement of the new methodology with respect to previous ones [21,27,32–34] comes from the fact that previous energy computation methodologies required the definition of intermediate parameters, while in the new methodology, the energy computation is solely based on the stationary probability distribution $\pi_c(i, k)$, $c = \{1, 2\}$.

As an example, Figure 13 shows the relative error of the average energy consumed by an SN per cycle in the *data* period in the scenario defined in Table 1. Relative values are obtained as $|x - y|/y$, where x is the value obtained by the analytical model, and y is the value obtained by simulation. Please note that P_{C1} and P_{C2} refer to the relative errors obtained using the previous methodology [23], while N_{C1} and N_{C2} refer to the relative errors obtained using the new methodology when measuring $E_{d,c}$, $c = \{1, 2\}$, for C1 and C2 SNs, respectively.

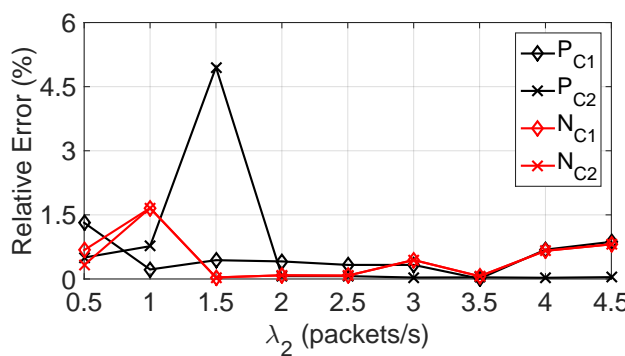


Figure 13. Average relative errors of the current and previous (Pre-method) energy computation methodologies.

Observe in Figure 13 that the relative errors represented for N_{C1} and N_{C2} are almost identical at each of the load points studied. Also, the relative errors represented for N_{C1} and N_{C2} have an homogeneous behavior with the load. Finally, we highlight that the relative errors of the new methodology are mostly below 1%, except for $\lambda_2 = 1$, where it is 1.5%,

However, the relative errors represented for P_{C1} and P_{C2} tend to have a less homogeneous behavior with the load than the relative errors obtained by the new methodology, and for $\lambda_2 = 1.5$, P_{C2} achieves a relative error larger than 4.5%.

6. Conclusions

A novel energy consumption model has been proposed for sensor nodes that deploy the synchronous duty-cycled MAC protocol named Priority Sink Access MAC (PSA-MAC) in heterogeneous IoT WSNs. The new methodology to determine the average energy consumed by SNs in a cycle considers all the operation modes in the entire operation cycle. The model is based on two 2D-DTMCs that define the evolution of the active sensor nodes of each class, as well as the number of packets in their queues. Their stationary probability distributions are used to derive, in a systematic and conceptually simple way, closed-form expressions that allow to determine the average energy consumed by the sensor nodes along an operating cycle.

The model considers different classes of SNs, each with its own features and priority assignments, allowing the determination of the performance of complex heterogeneous WSNs. In addition, each class can independently support two packet transmission modes: the single *DATA* packet transmissions (SPT), or the more sophisticated aggregate *DATA* packet transmission (APT) mode.

The model has been designed to be able to compute the energy consumed in every period of the cycle, the *sync* (synchronization), *data* and *sleep* periods. In addition, the model considers *normal* and *awake* operating cycles. During a *normal* cycle, an inactive sensor node will remain in the *sleep* mode for the full duration of the cycle once the *sync* period ends. However, at the end of a *sync* period, active sensor nodes will start contending for access to the channel. After an active sensor node transmits a packet frame successfully, or as soon as it detects a collision, it will switch to the *sleep* mode. An active sensor node also switches to the *sleep* mode as soon as it detects that it has lost the contention. However, during *awake* cycles, an SN, instead of switching to the *sleep* mode, will remain awake until the end of the cycle to hear possible transmissions of *SYNC* packets. The proposed model determines the average energy consumed by an SN in both *normal* and *awake* cycles.

The accuracy of the proposed methodology to determine the average energy consumed by a sensor node in a cycle has been measured by comparing the results of the analytical model to those obtained by a customized discrete-event simulation program. The obtained results show that the approximate analytical model is very accurate.

In its current form, the model only considers ideal channels, i.e., an error-free channel from the MAC perspective. In a future work, we plan to extend the model to support a more realistic error-prone channel. This will allow the model to take into account the impact of the MAC layer, as well as the impact of the physical layer on the network performance.

Author Contributions: Conceptualization, C.P. and J.M.-B.; methodology, C.P. and J.M.-B.; software, C.P. and J.M.-B.; validation, C.P.; formal analysis, C.P., J.M.-B., V.P. and V.C.-G.; investigation, C.P.; resources, J.M.-B., V.P. and V.C.-G.; writing—original draft preparation, C.P., J.M.-B.; supervision, J.M.-B., V.P. and V.C.-G.; funding acquisition, J.M.-B., V.P. and V.C.-G. All authors have read and agreed to the published version of the manuscript.

Funding: This work was supported through Grant PID2021-123168NB-I00, funded by MCIN/AEI, Spain/10.13039/501100011033 and the European Union A way of making Europe/ERDF, and Grant TED2021-131387B-I00, funded by MCIN/AEI, Spain/10.13039/501100011033 and the European Union NextGenerationEU/ RTRP. Canek Portillo was supported in part by Grant 2014-0870/001-001 (EuroinkaNet) and by Grant DSA/103.5/15/6629 (SEP-SES).

Data Availability Statement: Data are contained within the article.

Conflicts of Interest: The authors declare no conflicts of interest.

References

1. Mansour, M.; Gamal, A.; Ahmed, A.I.; Said, L.A.; Elbaz, A.; Herencsar, N.; Soltan, A. Internet of Things: A Comprehensive Overview on Protocols, Architectures, Technologies, Simulation Tools, and Future Directions. *Energies* **2023**, *16*, 3465. [[CrossRef](#)]
2. Ahmed, S. Energy Aware Software Defined Network Model for Communication of Sensors Deployed in Precision Agriculture. *Sensors* **2023**, *23*, 5177. [[CrossRef](#)] [[PubMed](#)]

3. Pedditi, R.B.; Debasis, K. Energy Efficient Routing Protocol for an IoT-Based WSN System to Detect Forest Fires. *Appl. Sci.* **2023**, *13*, 3026. [[CrossRef](#)]
4. Chi, H.R.; Wu, C.K.; Huang, N.; Tsang, K.; Radwan, A. A Survey of Network Automation for Industrial Internet-of-Things Toward Industry 5.0. *IEEE Trans. Ind. Inform.* **2023**, *19*, 2065–2077. [[CrossRef](#)]
5. Li, B.; Zhao, Q.; Jiao, S.; Liu, X. DroidPerf: Profiling memory objects on android devices. In Proceedings of the 29th Annual International Conference on Mobile Computing and Networking (MobiCom 2023), Madrid, Spain, 2–6 October 2023; pp. 1–15.
6. Raut, S.; Bhandari, C.; Jain, H. A Comparative Study of Power Optimization Techniques for Microcontroller based IoT Applications. In Proceedings of the 2024 Fourth International Conference on Advances in Electrical, Computing, Communication and Sustainable Technologies (ICAECT), Bhilai, Chhattisgarh, India, 11–12 January 2024; pp. 1–8.
7. Abdul-Qawy, A.; Alduais, N.; Saad, A.; Taher, M.; Nasser, A.; Saleh, S.; Khatri, N.B. An enhanced energy efficient protocol for large-scale IoT-based heterogeneous WSNs. *Sci. Afr.* **2023**, *21*, e01807. [[CrossRef](#)]
8. Abdulzahra, A.; Al-Qurabat, A.; Abdulzahra, S. Optimizing energy consumption in WSN-based IoT using unequal clustering and sleep scheduling methods. *Internet Things* **2023**, *22*, 100765. [[CrossRef](#)]
9. Banti, K.; Karampelias, I.; Dimakis, T.; Boulogeorgos, A.; Kyriakidis, T.; Louta, M. LoRaWAN Communication Protocols: A Comprehensive Survey under an Energy Efficiency Perspective. *J. Telecom.* **2022**, *3*, 322–357. [[CrossRef](#)]
10. Ghaderi, M.R.; Amiri, N. LoRaWAN sensor: Energy analysis and modeling. *Wirel. Netw.* **2024**, *30*, 1013–1036. [[CrossRef](#)]
11. Correia, F.; Alencar, M.; Assis, K. Stochastic Modeling and Analysis of the Energy Consumption of Wireless Sensor Networks. *IEEE Lat. Am. Trans.* **2023**, *21*, 434–440. [[CrossRef](#)]
12. Nguyen, M.T.; Nguyen, H.M.; Masaracchia, A.; Nguyen, C.V. Stochastic-Based Power Consumption Analysis for Data Transmission in Wireless Sensor Networks. *EAI Endorsed Trans. Ind. Netw. Intell. Syst.* **2019**, *6*, e5. [[CrossRef](#)]
13. Xu, D.; Wang, K. Stochastic Modeling and Analysis with Energy Optimization for Wireless Sensor Networks. *Int. J. Distrib. Sens. Netw.* **2014**, *10*, 672494. [[CrossRef](#)]
14. Rahimifar, A.; Kavian, Y.; Kaabi, H.; Soroosh, M. Predicting the energy consumption in software defined wireless sensor networks: a probabilistic Markov model approach. *J. Ambient. Intell. Humaniz. Comput.* **2021**, *12*, 9053–9066. [[CrossRef](#)]
15. Zhang, Y.; Li, W. Energy consumption analysis of a duty cycle wireless sensor network model. *IEEE Access* **2019**, *7*, 33405–33413. [[CrossRef](#)]
16. Xiao, W.; Kaneko, M.; El Rachkidy, N.; Guitton, A. Integrating lora collision decoding and mac protocols for enabling iot massive connectivity. *IEEE Internet Things Mag.* **2022**, *5*, 166–173. [[CrossRef](#)]
17. Wang, Y.; Vuran, M.C.; Goddard, S. Stochastic Analysis of Energy Consumption in Wireless Sensor Networks. In Proceedings of the 2010 7th Annual IEEE Communications Society Conference on Sensor, Mesh and Ad Hoc Communications and Networks (SECON), Boston, MA, USA, 21–25 June 2010; pp. 1–9.
18. Galluccio, L.; Palazzo, S. End-to-End Delay and Network Lifetime Analysis in a Wireless Sensor Network Performing Data Aggregation. In Proceedings of the 2010 In 2009 IEEE Global Telecommunications Conference (GLOBECOM 2009), Honolulu, HI, USA, 30 November–4 December 2010; pp. 1–6.
19. Li, Z.; Peng, Y.; Qiao D.; Zhang, W. Joint Aggregation and MAC design to prolong sensor network lifetime. In Proceedings of the 2013 21st IEEE International Conference on Network Protocols (ICNP), Goettingen, Germany, 7–10 October 2013; pp. 1–10.
20. Li, Z.; Peng, Y.; Qiao D.; Zhang, W. LBA: Lifetime balanced data aggregation in low duty cycle sensor networks. In Proceedings of the 31st Annual IEEE International Conference on Computer Communications (IEEE INFOCOM 2012), Orlando, FL, USA, 25–30 March 2012; pp. 1844–1852.
21. Guntupalli, L.; Martinez-Bauset, J.; Li, F.Y.; Weitnauer, A. Aggregated packet transmission in duty-cycled WSNs: Modeling and performance evaluation. *IEEE Trans. Veh. Technol.* **2016**, *66*, 563–579. [[CrossRef](#)]
22. Portillo, C.; Martinez-Bauset, J.; Pla, V.; Casares-Giner, V. Energy Modeling and Analysis for IoT Sensor Devices: A DTMC-Based Approach. In Proceedings of the Workshop on Innovation on Information and Communication Technologies (ITACA-WIICT 2018), Valencia, Spain, 13 July 2018; pp. 126–142.
23. Portillo, C.; Martinez-Bauset, J.; Pla, V.; Casares-Giner, V. Modeling of Duty-Cycled MAC Protocols for Heterogeneous WSN with Priorities. *Electronics* **2020**, *9*, 467. [[CrossRef](#)]
24. Portillo, C.; Martinez-Bauset, J.; Pla, V.; Casares-Giner, V. Heterogeneous WSN Modeling: Packet Transmission with Aggregation of Traffic. In Proceedings of the Interdisciplinary Conference on Mechanics, Computers and Electrics (ICMECE 2022), Barcelona, Spain, 6–7 October 2022; pp. 278–283.
25. Pereira, F.; Correia, R.; Carvalho, N.B. Comparison of active and passive sensors for IoT applications. In Proceedings of the 2018 IEEE Wireless Power Transfer Conference (WPTC), Montreal, QC, Canada, 3–7 June 2018; pp. 1–3.
26. Guntupalli, L.; Martinez-Bauset, J.; Li, F.Y. Performance of Frame Transmissions and Event-triggered Sleeping in Duty-Cycled WSNs with Error-Prone Wireless Links. *Comput. Netw.* **2018**, *134*, 215–227. [[CrossRef](#)]
27. Martinez-Bauset, J.; Guntupalli, L.; Li, F.Y. Performance analysis of synchronous duty-cycled MAC protocols. *IEEE Wirel. Commun. Lett.* **2015**, *4*, 469–472. [[CrossRef](#)]
28. Portillo, C.; Martinez-Bauset, J.; Pla, V.; Casares-Giner, V. The State Transition Probabilities of the Two 2D-DTMC with Traffic Aggregation. Technical Note. Available online: https://drive.google.com/drive/folders/1ezmxQxjrt410T_GglqUo6YWKgOEJKd1M?usp=sharing (accessed on 10 June 2024).

29. MICAz Data Sheet. Crossbow Technology Incorporated, San Jose, CA, USA. Available online: http://courses.ece.ubc.ca/494/files/MICAz_Datasheet.pdf (accessed on 1 April 2024).
30. Zhang, S. Modeling, Analysis and Design of Energy Harvesting Communication Systems. Ph.D. Thesis, University of Rochester, Rochester, NY, USA, 2013.
31. Kramer, M.; Gerald, A. *Energy Measurements for Micaz Node*; Technical Report KrGe06; University of Kaiserslautern: Kaiserslautern, Germany, 2006; pp. 1–6.
32. Yang, O.; Heinzelman, W. Modeling and throughput analysis for SMAC with a finite queue capacity. In Proceedings of the 2009 International Conference on Intelligent Sensors, Sensor Networks and Information Processing (ISSNIP), Melbourne, Australia, 7–10 December 2009; pp. 409–414.
33. Yang, O.; Heinzelman, W. Modeling and performance analysis for duty-cycled MAC protocols with applications to S-MAC and X-MAC. *IEEE Trans. Mob. Comput.* **2012**, *11*, 905–921. [[CrossRef](#)]
34. Portillo, C.; Martinez-Bauset, J.; Pla, V. Modelling of S-MAC for Heterogeneous WSN. In Proceedings of the 2018 9th IFIP International Conference on New Technologies, Mobility and Security (NTMS), Paris, France, 26–28 February 2018; pp. 1–6.

Disclaimer/Publisher’s Note: The statements, opinions and data contained in all publications are solely those of the individual author(s) and contributor(s) and not of MDPI and/or the editor(s). MDPI and/or the editor(s) disclaim responsibility for any injury to people or property resulting from any ideas, methods, instructions or products referred to in the content.